Fibroblast Adhesion to RGDS Shows Novel Features Compared with Fibronectin

Heather B. Streeter and David A. Rees

National Institute for Medical Research, Mill Hill, London NW7 1AA, United Kingdom

Abstract. As previously shown by others, the fibroblast attachment and spreading activity of fibronectin is mimicked by a short peptide (RGDS or longer) from the cell binding domain. Normal rat kidney fibroblasts showed similar attachment kinetics on either peptide GRGDSC or bovine plasma fibronectin and binding to either substratum was inhibited by peptide alone. We now demonstrate, however, considerable differences in biological activity between peptide and fibronectin. In particular, cells developed novel adhesion structures on peptide-coated substrata. Interference reflection microscopy showed a predominance of small round dark grey/black patches of adherent membrane ("spots") with relatively few focal adhesions, which occurred only at the outermost cell margins in contrast to their distribution in cells spread on fibronectin. The spots were resistant to detergent extraction and stained less strongly or not at all for vinculin. Electron microscopy in vertical thin section showed that the ventral surface of the cell was characterized by "point-contacts", corresponding in size to the spot structures seen by interference reflection microscopy, and which were only occasionally associated with microfilaments. Cells also required a higher substratum loading of peptide than fibronectin to promote spreading and proceeded to spread less rapidly and to a lesser extent, developing very few and extremely fine actin cables.

THE interaction of cells with extracellular matrix is important for the regulation of cellular growth, migration, and differentiation (17). One of the major glycoproteins of the extracellular matrix is fibronectin, which consists of several protease-resistant domains, each of which contains specific binding sites for other extracellular molecules and for the cell surface (for review see reference 43). When fibroblasts are seeded on a fibronectin-coated substrate in serum-free medium, attachment and subsequent spreading are followed by reorganization of the cytoskeleton into stress fibres and the formation of focal adhesions.

Ruoslahti and co-workers (29–31) have located the cell attachment activity of fibronectin to a sequence as short as a tetrapeptide (RGDS) within the cell-binding domain close to the carboxyl-terminal heparin-binding domain. Substrate-bound peptide promoted fibroblast attachment and spreading, and soluble peptide added to the medium was able to inhibit both attachment and spreading on plasma fibronectin-coated surfaces (29, 44).

Fragments of the fibronectin molecule other than the cell binding domain do not support the attachment of secondary fibroblasts to substratum (42). However, their binding activities for such components as heparan sulphate (23), collagen, and fibrin, and the existence of a second cell-binding site thought to function in matrix assembly (26), suggest that regions of the fibronectin molecule, in addition to the primary cell-binding domain, might well play a role in extracellular organization and thus influence cell–substratum relationships. Heparan sulphate proteoglycan has been shown to colocalize with focal adhesions at the level of the light microscope in spread cells (40). Two recent reports have shown that proteolytically derived cell-binding domain alone cannot mimic the full activity of fibronectin in promoting formation of mature focal adhesions (20, 42). It is of interest also to determine the activity of short synthetic peptides that differ from native and isolated domains both in strength (5), and specificity (33) of binding to cells. We report for the first time that GRGDSC-mediated adhesion shows several novel features. These are in the morphology and composition of specialized adhesion structures, and in quantitative aspects of adhesion, spreading, and their inhibition.

Materials and Methods

Cell Culture

Normal rat kidney (NRK)[1] fibroblasts were routinely cultured in MEM containing 10% FCS (Sera Laboratories, Ltd., Crawley Down, Sussex, United Kingdom), penicillin (100 IU ml^{-1}) and streptomycin (0.1 mg/ml; Gibco Ltd., Uxbridge, Middlesex, United Kingdom) in a 95% air/5% CO_2 atmosphere.

Preparation of Substrata

Fibronectin was isolated and purified from bovine plasma essentially as previously described (39).

The peptide GRGDSC was prepared either as the dimer by the method of Merrifield (27, 15) or as the monomer by the method of Sheppard (6).

Dr. Streeter's present address is Department of Pediatrics, School of Medicine, Stanford University, Stanford, CA 94305.

1. *Abbreviations used in this paper*: NRK, normal rat kidney; SPDP, *N*-succinimidyl 3-(2-pyridyldithio) propionate.

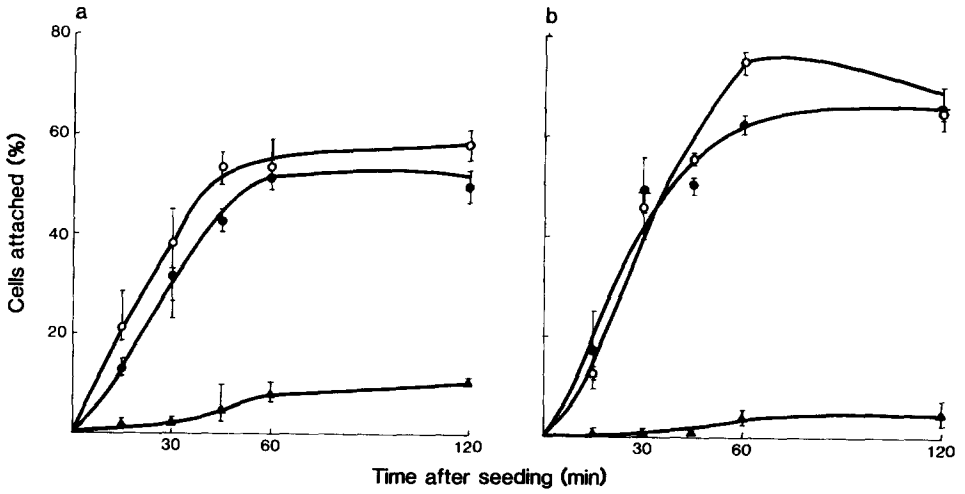

Figure 1. Rate of attachment of NRK fibroblasts on various substrata. Untreated cells (*a*) or cells pretreated with 50 μM emetine (*b*) and labeled with [^{35}S]methionine were trypsinized as described in Materials and Methods and seeded on substrata coated with fibronectin (*open circles*), BSA-GRGDSC (*solid circles*), or BSA-SPDP alone (reduced; *solid triangles*). At time points indicated, radioactivity associated with attached cells was counted (triplicate measurements) and expressed as a mean percentage of the total labeled cells seeded per well (bars represent maximum and minimum values).

Two other peptides, GRGDS and GRGES, used in inhibition of cell attachment experiments, were also prepared as by Sheppard. After cleavage from their respective resins, the peptides were purified on a Sephadex G-15 column (1.6 × 79.0-cm; Pharmacia, Uppsala, Sweden). Further purification of the Merrifield peptide, prepared as a dimer, was required. The dimer was loaded on an SP C-25 Sephadex column (1.0 × 43.0-cm; Pharmacia), eluted with a linear gradient 0–1 M NaCl in 0.05 M phosphate buffer, pH 4.0, and the peptide-containing peak was adjusted to pH 7.5 with a 1-M Tris solution. The other three peptides were lyophilized, resuspended in distilled water, and adjusted to pH 7.5 with NaOH. For attachment and spreading assays, substrata of fibronectin or peptide were made by coating either glass coverslips (for light microscopy; Chance Propper Ltd., Warley, United Kingdom), Melinex (for electron microscopy; I. C. I. Runcorn, Cheshire, United Kingdom), or tissue culture multiwell plates (Linbro, Flow Labs. Inc., Hertfordshire, United Kingdom). Fibronectin (0.05 ml of a 0.013 mg/ml solution in PBS) was added directly to a coverslip and allowed to adsorb overnight in a humid atmosphere at room temperature, washed with PBS, then incubated with heat-treated (80°C, 10 min) BSA (0.05 ml of a 1-mg/ml solution; Sigma Chemical Co. Ltd., Poole, Dorset, United Kingdom) for 15 min at 37°C. The GRGDSC substratum was made by coupling the COOH-terminal cysteine of the peptide to a BSA-coated surface with the hetero-bifunctional cross-linker *N*-succinimidyl 3-(2-pyridyldithio) propionate (SPDP; Pharmacia). BSA was derivatized with SPDP by the procedure recommended by the manufacturer and concentrated to 12 mg/ml; aliquots (0.05 ml) were added to coverslips for 16 h at room temperature. After washing the BSA-SPDP-coated surface with PBS, 0.05 ml of a GRGDSC solution (0.23 μmol/ml of monomer; or, when dimer was used, 0.05 ml of 0.68 μmol/ml peptide prereduced with a twofold molar excess of dithiothreitol for 16 h) was allowed to cross-link for 16 h at room temperature.

For the control, a nonadhesive substratum was made by repeating the coupling procedure to a BSA-SPDP-coated surface as described above, omitting the peptide. Coated surfaces were finally rinsed with three washes of PBS. Coated tissue culture wells were prepared as described above for coverslips, keeping the ratio of added protein (or peptide) to surface area constant.

For experiments estimating protein bound to coverslips, fibronectin and BSA were iodinated as in reference 14. ^{125}I-fibronectin was diluted with cold fibronectin to a final specific activity of 0.55 mCi/mg. The maximum number of SPDP groups available for cross-linking peptide was estimated from the radioactivity associated with a coverslip after adsorption of SPDP-substituted ^{125}I-BSA (diluted with cold BSA; final specific activity 2 μCi/mg). The number of SPDP molecules cross-linked per mole ^{125}I-BSA was measured spectrophotometrically (16, 35).

Attachment Assays

Cells near confluency were prelabeled for 2 h with 20 μCi/ml [^{35}S]methionine (Amersham International, Amersham, Buckinghamshire, United Kingdom) in methionine-free DME (Gibco Ltd., Uxbridge, Middlesex, United Kingdom) containing 10% FCS. Labeled cells, either treated or untreated with emetine (50 μM in MEM containing 10% FCS for 2 h at 37°C, Sigma) were then detached from the flask with 0.125% trypsin (Difco Laboratories, Surrey, United Kingdom), 0.01% Na_2 EDTA and suspended in 10 ml serum-free medium (MEM) with penicillin and streptomycin containing 0.1 mg/ml soybean trypsin inhibitor. After centrifugation, the cells were washed with 10 ml MEM and finally resuspended in MEM containing 2 mg/ml BSA at a concentration of 0.25 × 10^6 cells/ml.

Aliquots (0.1 ml) of this suspension were seeded on individual substratum-coated wells of the multiwell plate and incubated for 15 min to 2 h at 37°C in a 95% air/5% CO_2 atmosphere. At various time points, nonattached cells were removed by gentle resuspension and wells were rinsed twice with 0.1 ml of MEM. An SDS solution (10% wt/vol; 0.1 ml) was added to each well for 1 h at 37°C to solubilize attached cells from the substratum. The radioactivity in each fraction was quantitated in a scintillation counter (Beckman-RIIC Ltd., High Wycombe, Buckinghamshire, United Kingdom) using Liquiscint (National Diagnostics, Inc., Somerville, NJ) as scintillation cocktail. As discussed in reference 12, this assay was meaningful only as a comparison between cell attachments to different proteins or peptides. Attachment assays were also performed in the presence of competing peptide, repeating the above procedure except that peptides GRGDS or GRGES were included in the final resuspension medium in increasing concentrations from 0.25 to 2.0 mM. Radioactivity associated with attached and nonattached fractions were quantitated after 1 h from the time of seeding.

Spreading Assay

Near confluent, unlabeled cells were detached and resuspended essentially as described above. Aliquots (0.05 ml) of a cell suspension of 2 × 10^6 cells/ml were plated either on 10-mm diameter glass coverslips or 1.0 × 1.0-cm Melinex squares and incubated for 30 min at 37°C in a 95% air/5% CO_2 atmosphere, after which a further 1 ml of MEM was added to each well. After 5 h, cells were examined either live or after fixation.

Microscopy

For light microscopy, cells were observed on a Leitz Ortholux II microscope fitted with interference reflection, epifluorescence, and phase-contrast objectives.

For interference reflection studies, cells were viewed either live or after fixation with 3% glutaraldehyde (TAAB Laboratories, Reading, Berks, United Kingdom) in 0.1 M sodium cacodylate buffer, pH 7.25.

F-actin was visualized by fluorescence labeling with nitrobenzoxadiazole phallacidin (Molecular Probes, Inc., Junction City, OR) after fixation of cells with 4% paraformaldehyde in PBS and permeabilization with 0.1% NP-40, 0.15 M NaCl, 1 mM Na_2EDTA, 20 mM Tris-HCl, pH 7.4. The staining procedure used was that suggested by the manufacturer.

Indirect immunofluorescence labeling of cells for vinculin (anti-mouse monoclonal, diluted 1:10; Bio Yeda, P. & S. Biochemicals Ltd., Liverpool, United Kingdom) was performed on spread fibroblasts after a short extraction with 0.5% Triton X-100 in PBS (10 min) and then fixation with 3% formaldehyde in PBS (10 min) at 20°C. Antibodies were applied for 1 h at 20°C diluted in 1% BSA, Tris-buffered saline. A secondary antibody, rabbit anti-mouse (1:500) was followed by fluorescein-coupled goat anti-rabbit (1:100). Before each antibody addition, coverslips were washed with 1%

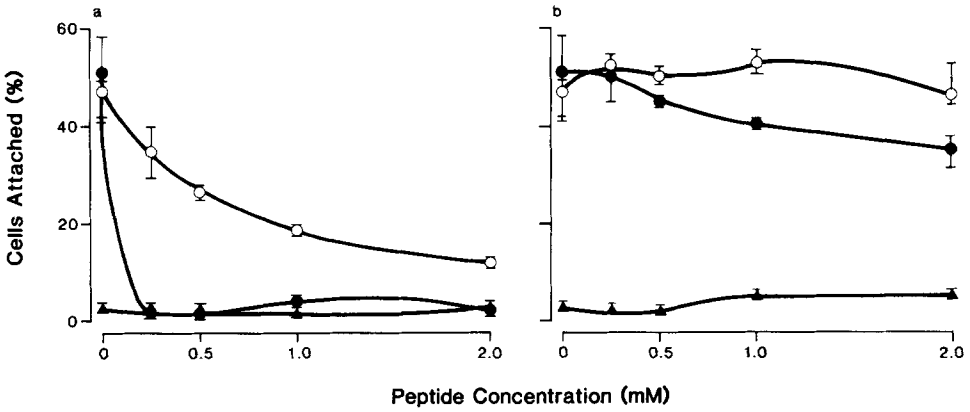

Figure 2. Inhibition of cell attachment to fibronectin or GRGDSC by soluble peptides in assay medium. NRK cells were pretreated with 50 μM emetine, labeled with [^{35}S]methionine, trypsinized (see Materials and Methods), resuspended in serum-free medium containing increasing concentrations of GRGDS (*a*) or GRGES (*b*), and plated onto fibronectin (*open circles*), BSA-GRGDSC (*solid circles*), or BSA-SPDP (control, *solid triangles*) substrata. At the soluble peptide concentrations indicated, radioactivity associated with attached and nonattached cells was quantitated 1 h after plating and expressed as described in Fig. 1.

BSA/Tris-buffered saline. For control experiments, a nonrelevant monoclonal antibody or preimmune rabbit IgG was used at the appropriate dilution and showed neglible labeling.

Cells for electron microscopy were fixed in 1.25% glutaraldehyde, 1% paraformaldehyde in 0.1 M sodium cacodylate buffer, pH 7.25, overnight and postfixed in 1% osmium tetroxide in the same buffer for 1 h. Cells were prestained with 1% aqueous uranyl acetate en bloc and dehydrated in a graded series of ethanols followed by embedding in araldite CY212. Thin sections were cut on an ultramicrotome (Reichert Jung Ltd., Cambridge Instruments, Cambridge, United Kingdom) stained with uranyl acetate and Reynolds' lead citrate (34) and viewed on a Philips 300 electron microscope.

Measurement of Fibroblast Spread Area

The spread area of fibroblasts attached to various substrata was measured and computed from photographic images of the cells. Cells were fixed with 3% glutaraldehyde, 0.1 M sodium cacodylate buffer, pH 7.25, and stained with haematoxylin. A high contrast cell image was obtained by photography with Kodak Technical Pan 2415 (rated at 40 A.S.A.; Kodak Ltd., Liverpool, United Kingdom) and Kodak No. 58 filter using brightfield microscopy to visualize the stained cells. The apparatus consisted of a British Broadcasting Corporation model B microcomputer (Acorn Computers Ltd., Cambridge, United Kingdom) with a Grafpad digitizing tablet connected to the user port and an Eltime R.16.4.2/RBH television picture store connected to the 1 MHz bus. An Hitachi KP120/E CCD TV camera produced the video input to the Eltime store and an Hitachi M173 E/R monochrome TV displayed the output (all from Samuelson Video Equipment, London, United Kingdom). The digitizer tablet was used to guide a rectangle adjusted to superimpose and encompass each cell image. The program, written for our purposes by John Satchell of The National Institute for Medical Research, used density information to calculate area and perimeter in units of pixels per mm^2. The system was precalibrated using an object of known area and a calibration factor was applied to all measurements. Consistent exposure of the photographic images to the camera was ensured by monitoring the video voltage level from the camera using an oscilloscope. Computation of cell area and perimeter was initiated from the keyboard by choosing the appropriate key to classify the cell shape. The program automatically rejected cell images which had been partly or wholly measured previously. Other errors in image detection were cancelled manually.

Results

Kinetics of Cell Attachment

NRK fibroblasts seeded onto multiwell dishes precoated with fibronectin or GRGDSC attached rapidly and with similar kinetics. Within 30 min, 37 and 31% of added cells attached to fibronectin and GRGDSC, respectively, reaching maximum cell attachment on both substrata 1 h after seeding (Fig. 1 *a*). BSA was included in the plating medium to depress nonspecific attachment.

A slightly greater rate of cell attachment was observed on the fibronectin substratum, reaching a plateau of attachment earlier (45 min) than GRGDSC (60 min). At no single time point was the difference in cell attachment numbers >8%, however. In an attempt to remove complications caused by, for example, the secretion of endogenous fibronectin, inhibition of protein synthesis and clearance of existing pools of fibronectin (9, 10) was achieved by preincubating [^{35}S]methionine-labeled fibroblasts with emetine for 1 h before trypsinization. During the assay period, 97% of protein synthesis was inhibited, as measured by the cell-associated TCA-precipitable counts. In the absence of protein synthesis, the slight increase in cell attachment rate on fibronectin as compared with GRGDSC was abolished and the time taken for maximal cell attachment was the same on both substrata (1 h; Fig. 1 *b*).

A GRGDSC-substituted surface was estimated to carry 4.85 nmol/cm^2 of peptide, on the basis of complete efficiency of coupling. (The coupling method used is reported [29] to be capable of achieving >85% efficiency.) Serial dilutions demonstrated that a 4-fold reduction in peptide added (from 0.23 to 0.06 μmol/ml) to SPDP-derivatized BSA-coated surface maintained cell attachment but not cell spreading and that a 10-fold reduction abolished attachment altogether. On a fibronectin-coated substratum, comparable attachment kinetics were observed when the substratum loading was very much lower, equivalent to 4.5×10^{-5} nmol/cm^2 (data established with ^{125}I-fibronectin).

Specificity of the GRGDS Sequence in Promoting Cell Attachment

Cell attachment to either GRGDSC-substituted or fibronectin substratum were both inhibited by the presence of pentapeptide GRGDS in the assay medium (Fig. 2 *a*). Under our experimental conditions, with the minimal substrata loadings to induce cell attachment and spreading, the amount of competing GRDGS required for half-maximal inhibition was 10-fold greater for a fibronectin (1.16 mM) than for a GRGDSC (0.1 mM) surface. Although addition of soluble GRGDS (2.0 mM) resulted in 80% inhibition of attachment

Table I. Spread Areas Attained by NRK Fibroblasts on Various Substrata

Substratum	Area of spread cells	Shape (percent of attached cells)					
		Kite	Square	Triangular	Oval	Bipolar	Round
	μm^2						
Fibronectin	6993 (2851)*	43.1	29.3	17.2	6.9	3.4	0
GRGDSC	4967 (1758)	17.4	21.1	32.1	21.2	3.7	4.5
BSA-SPDP	2158 (788)	0	3.2	3.2	7.6	0.6	85.4

Cells were allowed to spread for 5 h before fixation and staining with haematoxylin. Cell areas of photographic images of stained cells were measured and computed as described in Materials and Methods. Description of cell shape (classified visually) was stored with the computed measurement. Data collected from two experiments, sample number: $n = 200$ (fibronectin); $n = 111$ (peptide); $n = 157$ (BSA-SPDP).
* Standard deviation shown in parentheses.

to fibronectin, this concentration of the closely related peptide GRGES had little effect (Fig. 2 *b*). Likewise, the inhibitory activity of GRGES on fibroblasts adhering to GRGDSC was minimal compared with that of GRGDS. The inactivity of GRGES and the extent of inhibition by GRGDS suggest that cell spreading events (as described below) on both GRGDSC and fibronectin surfaces can be attributed to initial attachment via the GRGDS sequence.

Comparison of Cell Spreading and Actin Distribution on Fibronectin and Peptide Substrata

Despite the similar rates of attachment on the two substrata, NRK fibroblasts spread much more slowly on GRGDSC than on fibronectin. As early as 2 h from time of plating, cells on fibronectin attained a spread area of ~85–90% of the final area as measured after 5 h, whereas on peptide they reached only 71% after 5 h (Table I). Cells spread on fibronectin were dominated by kite- and square-shaped cells (72.4% of attached cells), whereas fewer of these shapes were noted on peptide (38.5% of attached cells) with an increase in triangular and oval spread cells (Table I).

Fluorescence microscopy demonstrated that fibroblasts fully spread on fibronectin were characterized by regular, straight, and abundant cables of F-actin (Fig. 3 *a*), terminating in focal adhesions. In contrast, cells spread for 5 h on GRGDSC contained very few and extremely fine actin cables which often ran close to the outer cell margins (Fig. 3 *b*).

Substratum Contact Structures on Fibronectin and Peptide

Cells fully spread in serum-free medium on a fibronectin-coated surface demonstrated typical focal adhesions (Fig. 4, *a* and *e*). In contrast, only 50% of NRK or chick embryo fibroblasts spread on GRGDSC demonstrated the presence of any such focal adhesions (Fig. 4, *b* and *f*) and these were fewer in number and mainly observed on the outer margins of the cells in areas of protruding lamellae. It is possible that some of this limited number of focal adhesions derived from the influence of endogenous fibronectin. Attempts to deplete this pool by preincubation with emetine unfortunately also eliminated the formation of any recognizable adhesion structures (the interference reflection microscopy image was uniformly grey, see Fig. 4 *d*), perhaps by blocking the regeneration of trypsin-damaged cell surface receptors. The interference reflection image of cells spread on GRGDSC was distinguished by a mottled appearance, which, on closer examination (Fig. 4, *b* and *f*), was seen to be composed of abundant dark grey/black structures, ranging in diameter from 115 to 240 nm, surrounded by small white areas of membrane. In cells spread on fibronectin similar spotlike structures were observed in much lower frequency and were either limited to the region of the cell beneath the nucleus or to the active edge of lamellae.

The spot structures remained even after cell extraction with 0.5% Triton X-100 (Fig. 5, *a* and *c*) and many failed

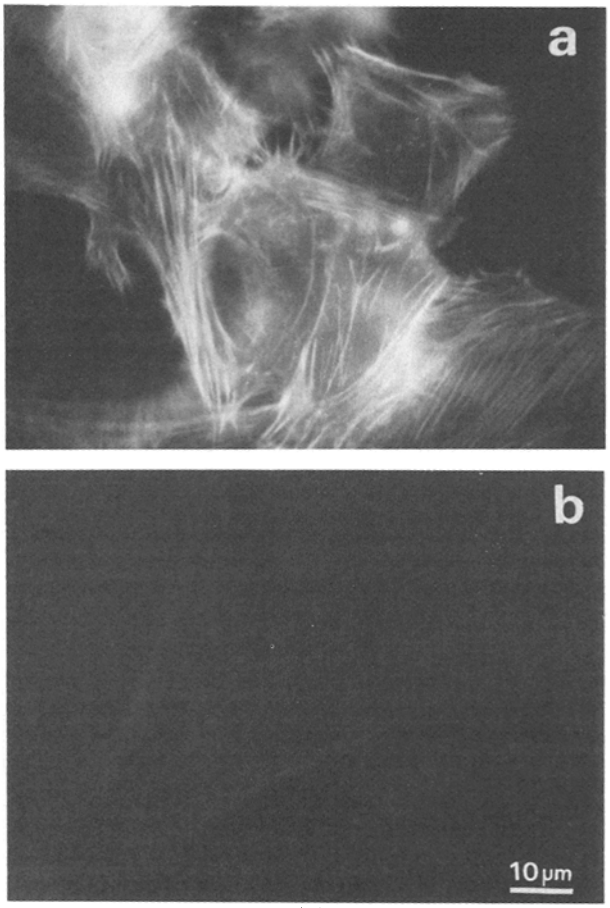

Figure 3. Actin organization in fibroblasts spread on fibronectin (*a*) or GRGDSC (*b*). Cells spread on either substratum were fixed and permeabilized after 5 h and F-actin was fluorescently labeled with nitrobenzoxadiazole phallicidin. Very few actin cables were observed in cells spread on peptide (*b*). Exposure time for both frames was 1 min.

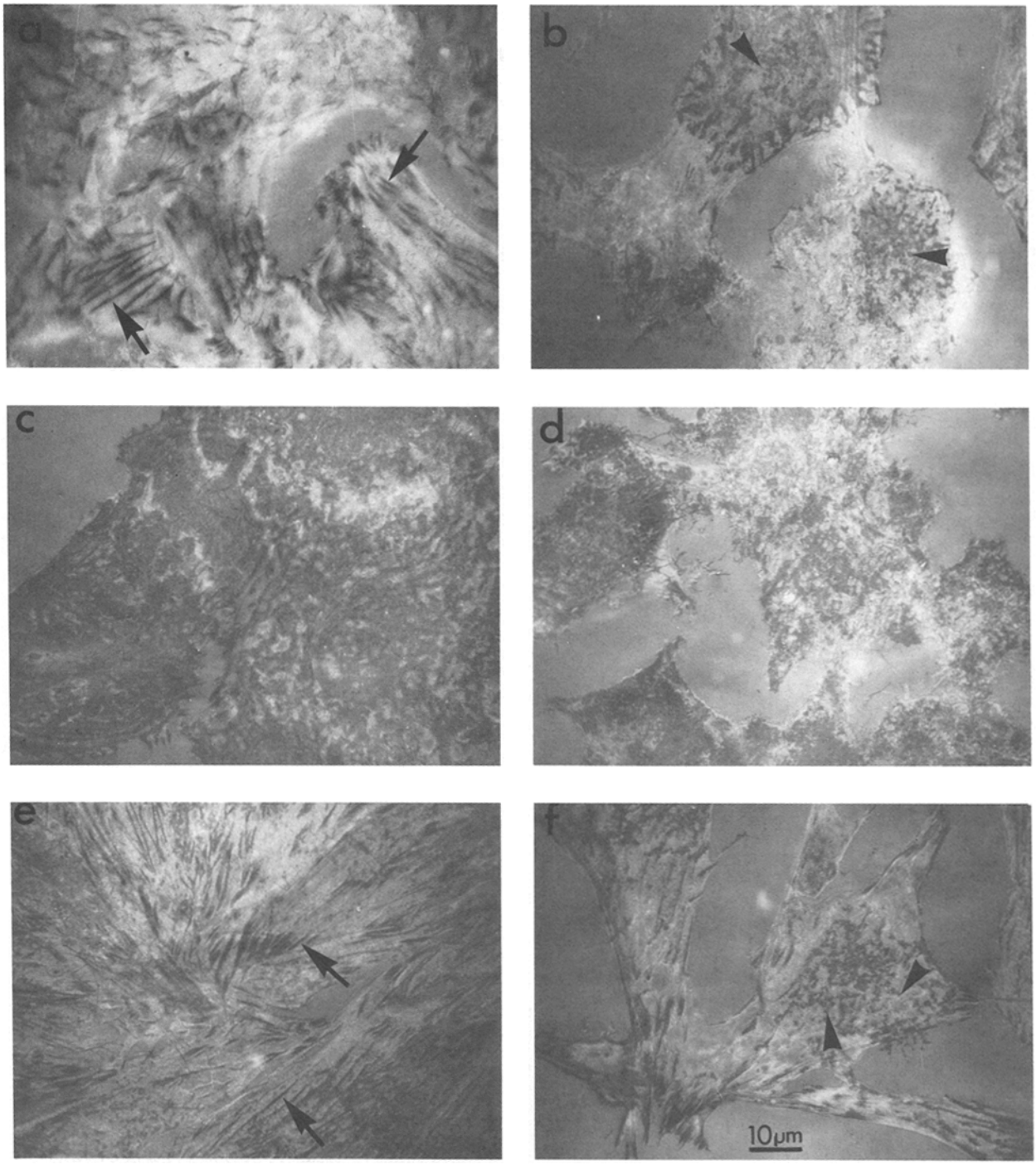

Figure 4. Interference reflection images of cells spreading on various substrata. NRK fibroblasts (*a–d*) and chick embryo fibroblasts (*e* and *f*) were allowed to spread on fibronectin (*a*, *c*, and *e*) or GRGDSC (*b*, *d*, and *f*) substrata for 5 h. Cells spread on fibronectin (*a* and *e*) demonstrated typical focal adhesions (*black arrows*), while GRGDSC-spread cells (*b* and *f*) were characterized by spotlike adhesion structures (*arrowheads*). After pretreatment of NRK fibroblasts with 50 μM emetine for 2 h before trypsinization, adhesions were destroyed on both fibronectin and GRGDSC surfaces (*c* and *d*).

to stain for vinculin (Fig. 5, *b* and *d*). Those spot structures having more dense interference reflection microscopy images, however, generally showed weak staining for vinculin (Fig. 5, *b* and *d*). As expected, vinculin staining was observed at the positions of focal adhesions in cells spread on either substrata (Fig. 5).

In five replicate experiments, the interference reflection microscopy observation of individual NRK fibroblasts indicated that the duration of both focal adhesions and spots was quite variable with no obvious differences in lifetime between either type of adhesive structure on fibronectin or GRGDSC substrata (Table II). Short-lived adhesions (10–30 min) were characteristic on both substrata, which either modified in shape and direction or disappeared within this

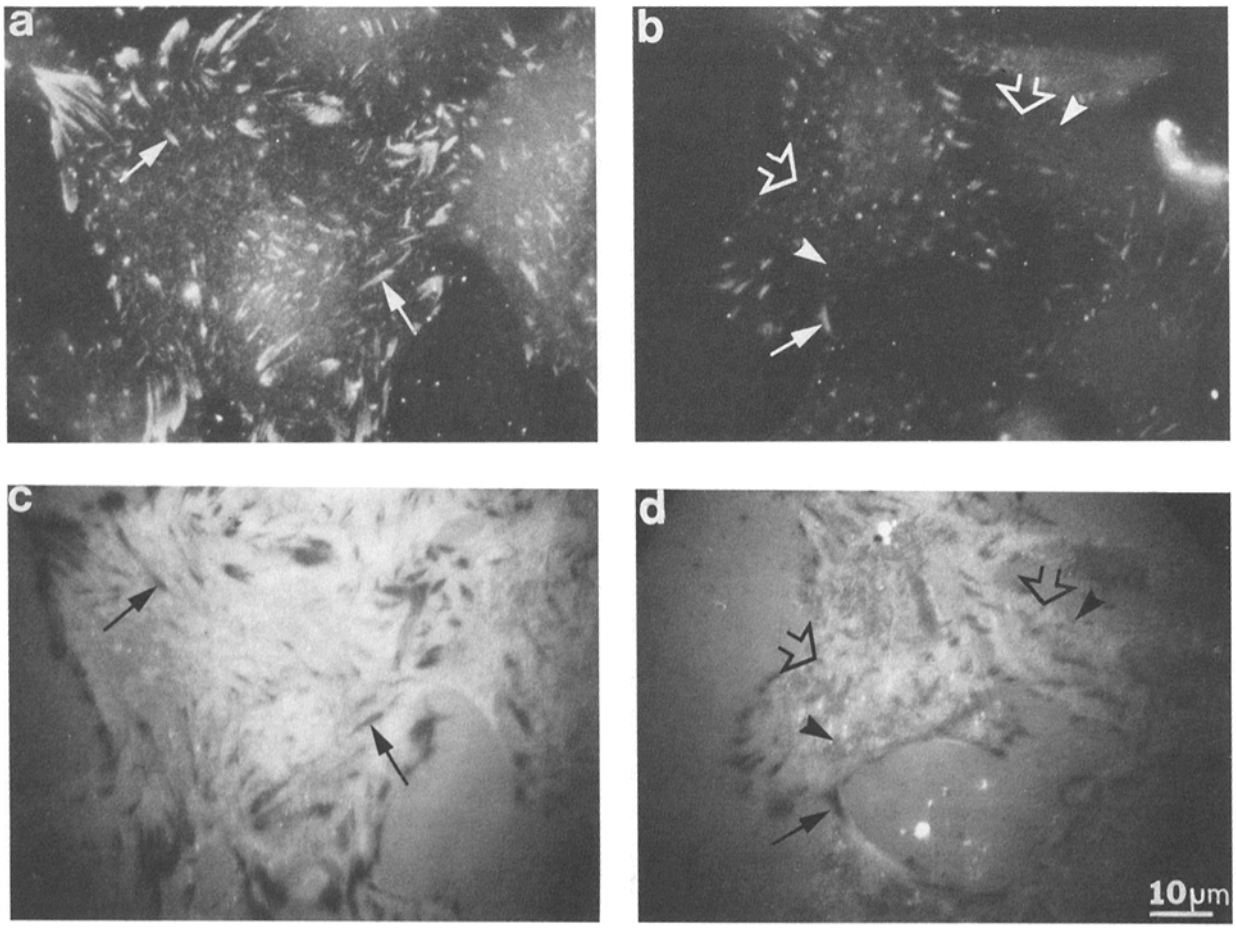

Figure 5. Indirect immunofluorescence labeling of adhesive structures formed on either fibronectin (*a* and *c*) or GRGDSC (*b* and *d*) for vinculin. Spread NRK fibroblasts were extracted briefly with detergent before fixation. Material remaining associated with the substratum was then probed with vinculin antibody (*a* and *b*) (see Materials and Methods). Visualization of the ventral surface of cells by interference reflection microscopy showed that both spot structures (*arrowheads* and *open arrows* in *d*) and focal adhesions (*arrows* in *c* and *d*) were resistant to detergent extraction. Correlation of vinculin staining with adhesive structures demonstrates that focal adhesions always label with vinculin (*arrows* in *a* and *c*, *b* and *d*); some spot structures also label with less intensity (*open arrows* in *b* and *d*). However, other spot structures are not vinculin-positive (*arrowheads* in *b* and *d*).

time. Some focal adhesions remained the same size and shape but changed direction within 15 min and continued to do so for 1–2 h. Other adhesions (both focal adhesions and spots) were longer-lived, from 30 min to 3–4 h.

Ultrastructure of Spread Cells

Electron microscopy in vertical thin section of fibroblasts demonstrated three major differences between cells spread on fibronectin and GRGDSC substrata. First, on GRGDSC the microfilament bundles associated with the ventral surface were fewer, thinner in diameter, and less tightly bundled than those in cells spread on fibronectin (Fig. 6, *a* and *b*). Second, a striking difference on GRGDSC was the predominance of a pattern characterized by "point" contacts (Fig. 6 *b*). These point contacts differed from mature focal adhesions both in that the area of contacting membrane was very much smaller (diameter at a distance of 15 nm from substratum, the distance which corresponds to black images in interference reflection [1, 19], was in the range 90–200 nm) and in that microfilaments were largely absent (Fig. 6 *b*). When microfilaments were associated with these structures, they turned down infrequently into the contact towards the substratum as in classical focal adhesions and were much more loosely organized. Dense submembraneous plaques such as are characteristic of focal adhesions were not observed in point contacts, although a few of these contacts (mainly those with some microfilament association) did show an increase in density after staining with either uranyl acetate or ruthenium red (data not shown). Third, the noncontacting areas of the ventral membrane appeared to be more irregular on GRGDSC than on fibronectin, and the distance of the membrane from the substratum between point contacts was generally greater (145–160 nm) than normally observed between focal adhesions (30–80 nm).

Statistical analysis (Student's *t*-test) revealed that the difference between the number of point contacts in cells spread on the two substrata was highly significant (data collected from two experiments, thin sections cut from 20–25 cells per substratum, $n = 170$, $t_{0.1\%}$–3.291). This analysis suggests that the point contact structure is a significant and common feature in cells spread on GRGDSC.

Table II. Lifetimes of Adhesive Structures in NRK Fibroblasts Seeded on Fibronectin or Peptide Substrata

Substratum	Adhesive structure	Time from seeding 2 h	3 h	4 h	5 h
Fibronectin*	Focal adhesion				
	1	——			
	2	——			
	3	——			
	4	——			
	5	——	——	——	——
GRGDSC‡	Focal adhesion				
	a	——			
	b	——	——		
	c	——	——		
	d	——	——		
	e	——	——	——	——
Fibronectin*	Spot structure				
	6	——			
	7			——	——
	8			——	——
	9				——
	10			——	——
GRGDSC‡	Spot structure				
	f	——			
	g	——	——		
	h	——	——	——	
	i			——	
	j	——	——	——	——

Interference reflection images of cells were monitored and photographed at 15-min intervals for up to 5 h from time of plating. The duration of individual adhesive structures are charted as individual lines. Focal adhesion (No. 5) doubled in length at 3.5 h and began decreasing in area at 4.6 h. Spot structure (No. 10) developed into a focal adhesion at 4 h and changed direction at 4.6 h.
* Individual adhesive structures formed on fibronectin substratum: focal adhesions, 1–5; spot structures, 6–10.
‡ Individual adhesive structures formed on GRGDSC substratum: focal adhesions, a–e; spot structures, f–j.

Focal adhesions were observed by electron microscopy in cells spread on GRGDSC, but had a looser microfilament organization than those on fibronectin (not shown) and were variable in size and organization.

Discussion

The experiments described here confirm previous reports on the biological activity of the peptide sequence RGDS from the cell-binding domain of fibronectin. In addition they show several striking quantitative and qualitative differences between the cellular responses to peptide and to parent fibronectin. They extend other recently published studies (20, 22, 25, 42) of preparations of cell-binding domain derived proteolytically from fibronectin, which show that cell spreading stops short of the development of focal adhesions and the fully organized cytoskeleton. Our observations with a defined synthetic peptide substratum, RGDSC, demonstrate the presence of adhesion structures with novel features.

The kinetics of attachment of NRK fibroblasts on fibronectin or peptide substrata (Fig. 1) were similar. Evidence for the specificity of the GRGDS sequence in promoting cell attachment was the competitive inhibition of attachment by soluble GRGDS but not by the related peptide GRGES at the same concentrations. However, the apparent substratum loadings of peptide and of fibronectin required for efficient attachment differed by up to five orders of magnitude, and the concentration of competing soluble GRGDS for half-maximal inhibition differed between the two substrata by at least one order of magnitude. Possible reasons are discussed below. Recent experiments have shown that the peptide RGDS binds to the cell surface receptor for vitronectin (33) as well as to the fibronectin receptor (32), and, moreover, does so with higher affinity. However, the similarity in kinetics on peptide and fibronectin substrata which is maintained in the absence of protein synthesis, is consistent with

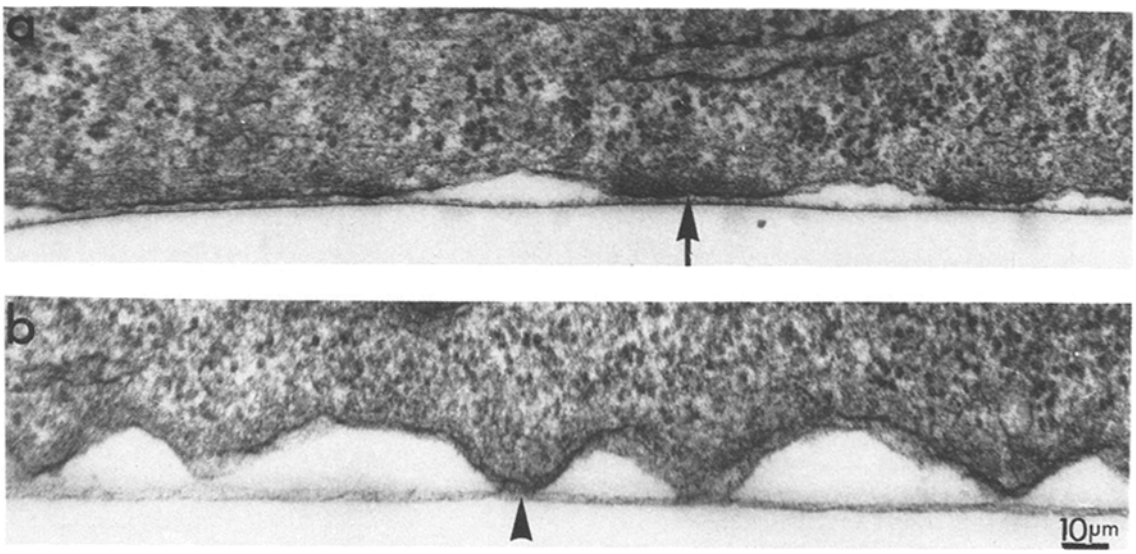

Figure 6. Electron micrographs in vertical thin section of the ventral surface of fibroblasts spread for 5 h on either a fibronectin or GRGDSC substratum. A typical focal adhesion seen on a fibronectin surface (*arrow* in *a*). In *b*, the ventral membrane is in contact with the GRGDSC substratum for a very short distance (90–200 nm), referred to in the text as point contact (*arrowhead*).

(though does not prove) the involvement of similar receptor mechanisms on both, especially since the vitronectin receptor is reportedly much more sensitive to trypsin (21).

Further differences in cellular response were seen in the events that followed initial attachment. Fibroblast spreading on peptide was slower than that on fibronectin and the degree to which cells finally spread was significantly less, with some differences in cell shape. Peptide is therefore less effective at stimulating the subsequent cytoskeletal activities involved in either promoting or stabilizing the final spread shape and additional mechanisms to the initial attachment interaction may be involved. Phallicidin staining and electron microscopy both showed that actin cables were much finer and rarer on peptide than on fibronectin substratum; individual microfilaments were also fewer and more disorganized. We suggest that these observations are mutually consistent. Since cell spreading is a dynamic process involving cycles of protrusion and retraction, the progressive consolidation of the actin cytoskeleton on fibronectin might limit retraction and so favor further spreading. On peptide, however, this mechanism of stabilization of the spread form does not operate, thus explaining why spreading always lags behind that on fibronectin.

Not unexpectedly, in view of the known association between actin cables and focal adhesions (2, 7, 18), interference reflection images of fibroblasts spread on fibronectin showed the classical pattern of numerous focal adhesions and prominent actin cables, whereas peptide-spread cells demonstrated fewer and less typical focal adhesions; these were always associated with the outermost margins of lamellapodia and we think it possible that their formation had been stimulated by endogenous (secreted) fibronectin. Cells spread on peptide typically showed a spotlike structure which persisted when viewed by interference reflection microscopy under illuminating conditions chosen to minimize images arising from higher order interference effects (8, 19). Thus, the image of the spot structure resulted from contact with the substratum. The spot structure was also resistant to detergent extraction of spread cells, as are other adhesive structures (Fig. 5, *a* and *c*). The dimensions of spot adhesions correlate with those of the point contacts we observed by electron microscopy (Fig. 4 and 6). This novel structure was not unique to NRK cells, since we have also observed it with baby hamster kidney and chick embryo fibroblasts spread on a peptide substratum. The point contact is of similar dimensions to the clathrin-associated membrane patches observed by electron microscopy of replicas of the inner surface of ventral membrane of NRK fibroblasts (28a). Some similarities also exist with the dot contacts observed by Neyfakh et al. and Vasiliev (references 28 and 38, respectively) on the leading edges of spreading fibroblasts; these are similar in size, rapidity of appearance, and lack of actin bundles. However, the dot contacts label positively for vinculin, which does not always seem to be the case for the spot adhesions. Based on these criteria, neither do the spot adhesions correspond to the podosomes found in Rous sarcoma virus–transformed cells (36).

The lifetimes of both spot contacts and focal adhesions, as studied in serum-free media by interference reflection microscopy, were often quite short, with some lasting only 10–15 min, suggesting that both types of adhesion structures are dynamic. This contrasts with earlier findings that focal adhesions in established cultures in serum are essentially permanent structures (11), except in particular phenotypes such as motile chick embryonic fibroblasts (13). It is of interest that the fluctuating pattern of focal contacts previously observed in an intermediate spread stage (stage 1) of fibroblasts on a chick serum glycoprotein was also in serum-free medium (37, 41). Time-lapse studies did not suggest the interconversion of point contacts and focal adhesions on peptide substrata, consistent with each type having arisen independently, e.g., the focal adhesion structures having been stimulated by endogenous fibronectin. In the absence of protein synthesis, attachment and spreading activities remained, but the ability to form either focal adhesions or spots was abolished (Fig. 4, *c* and *d*), presumably owing to proteolytic damage to additional cell surface features necessary for the formation of either type of specialized adhesive structure.

In summary, cell attachment and spreading on peptide have been found to differ relative to attachment and spreading on fibronectin in (*a*) substratum loading requirement; (*b*) susceptibility to competitive inhibition; (*c*) morphology of the adhesion structure; and (*d*) composition of the adhesion structure. The first two effects can no doubt be explained at least in part by the difference of two orders of magnitude in dissociate constants for receptor binding (3–5). The enormous difference in apparent receptor loading requirement, which is as great as five orders of magnitude, could reflect some combination of limited accessibility of the ligand, poor efficiency of coupling, and/or perhaps the existence of a cooperative element in the attachment mechanism to substrate-bound fibronectin (24) which is lacking for substrate-bound peptide. It is unlikely that the different susceptibilities to competitive inhibition can be explained simply in terms of a higher effective concentration of binding domains on the fibronectin substratum, since all experiments were performed at the limiting threshold concentration required for attachment and spreading. In view of recent evidence for fibroblasts of embryonic origin (42), interactions may be required with heparin-binding as well as cell-binding domains for focal adhesion development, in which case the morphological differences might be explained in terms of the absence of heparin/heparan sulphate–binding activity on the peptide relative to fibronectin substrata. On the other hand, it is reported that interactions with mixtures of cell-binding and heparin-binding fragments failed to induce focal adhesion formation in BALB/c 3T3 cells (20)

The authors wish to thank J. Satchell for a computerized method for cell area measurements, E. Hirst for electron microscopy, J. Charlton for fibronectin preparations, R. A. Faulkes and J. Charlton for peptide synthesis, and S. Lathwell for amino acid analysis.

Received for publication 16 February 1987.

Note added in proof. Since this paper went to press, we have seen the article by Singer et al. (1987, *J. Cell Biol.*, 104:573–584), which presents conclusions in apparent disagreement with our own. There is at present no obvious explanation. Three differences in experimental procedure were that Singer et al. used (*a*) polylysine coating of coverslips, (*b*) cell trypsinization in the presence of Ca^{2+}, and (*c*) incorporation of RGDS into a 13-mer sequence. In our hands, changes *a* and *b* do not facilitate focal contact formation (Smith, M. A., unpublished work).

References

1. Abercrombie, M., and G. A. Dunn. 1975. Adhesions of fibroblasts to substratum during contact inhibition observed by interference reflection microscopy. *Exp. Cell Res.* 92:57–62.
2. Abercrombie, M., J. E. M. Heaysman, and S. M. Pegrum. 1971. The loco-

motion of fibroblasts in culture. IV. Electron microscopy of the leading lamella. *Exp. Cell Res.* 67:359–367.
3. Akiyama, S. K., and K. M. Yamada. 1985. The interaction of plasma fibronectin with fibroblastic cells in suspension. *J. Biol. Chem.* 260: 4492–4500.
4. Akiyama, S. K., and K. M. Yamada. 1985. Synthetic peptides competitively inhibit both direct binding to fibroblasts and functional biological assays for the cell-binding domain of fibronectin. *J. Biol. Chem.* 260: 10402–10405.
5. Akiyama, S. K., E. Hasegawa, T. Hasegawa, and K. M. Yamada. 1985. The interaction of fibronectin fragments with fibroblastic cells. *J. Biol. Chem.* 260:13256–13260.
6. Atherton, E., C. J. Logan, and R. C. Sheppard. 1981. Peptide synthesis. Part 2. Procedures for solid-phase synthesis using N-fluorenylmethyloxycarbonylamino-acids on polyamide supports. Synthesis of substance P and of Acyl carrier protein 65–74 decapeptide. *J. Chem Soc. Perkin Trans. I.* 538–546.
7. Badley, R. A., A. Woods, L. Carruthers, and D. A. Rees. 1980. Cytoskeleton changes in fibroblast adhesion and detachment. *J. Cell Sci.* 43:379–390.
8. Bereiter-Hahn, J., C. H. Fox, and B. Thorell. 1979. Quantitative reflection contrast microscopy of living cells. *J. Cell Biol.* 82:767–779.
9. Bumol, T. F., and R. A. Reisfield. 1983. Biosynthesis and secretion of fibronectin in human melanoma cells. *J. Cell. Biochem.* 21:129–140.
10. Choi, M., and R. O. Hynes. 1979. Biosynthesis and processing of fibronectin in NIL. 8 hamster cells. *J. Biol. Chem.* 254:12050–12055.
11. Couchman, J. R., and D. A. Rees. 1979. The behaviour of fibroblasts migrating from chick heart explants: changes in adhesions, locomotion and growth, and in the distribution of actomyosin and fibronectin. *J. Cell Sci.* 39:149–165.
12. Couchman, J. R., M. Höök, D. A. Rees, and R. Timpl. 1983. Adhesion, growth, and matrix production by fibroblasts on laminin substrates. *J. Cell Biol.* 96:177–183.
13. Couchman, J. R., D. A. Rees, M. R. Green, and C. G. Smith. 1982. Fibronectin has a dual role in locomotion and anchorage of primary chick fibroblasts and can promote entry into the division cycle. *J. Cell Biol.* 93:402–410.
14. Fraker, P. J., and J. C. Speck, Jr. 1978. Protein and cell membrane iodinations with a sparingly soluble chloramide,1,3,4,6-tetrachloro-3a,6a-diphenylglycoluril. *Biochem. Biophys. Res. Commun.* 80:849–857.
15. Gisin, B. F. 1973. Preparation of Merrifield-resins through total esterification with cesium salts. *Helv. Chim. Acta.* 56:1476–1482.
16. Grassetti, D. R., and J. F. Murray. 1967. Determination of sulphydryl groups with 2,2′- or 4,4′-dithiopyridine. *Arch. Biochem. Biophys.* 119:41–49.
17. Hay, E. D., editor. 1982. Cell Biology of the Extracellular Matrix. Plenum Publishing Corp., New York. 417 pp.
18. Heath, J. P., and G. A. Dunn. 1978. Cell to substratum contacts of chick fibroblasts and their relation to the microfilament system. A correlated interference-reflexion and high-voltage electron-microscope study. *J. Cell Sci.* 29:197–212.
19. Izzard, C. S., and L. A. Lochner. 1976. Cell-to-substrate contacts in living fibroblasts: an interference reflexion study with an evaluation of the technique. *J. Cell Sci.* 21:129–159.
20. Izzard, C. S., R. Radinsky, and L. A. Culp. 1986. Substratum contacts and cytoskeletal reorganization of BALB/3T3 cells on a cell-binding fragment and heparin-binding fragments of plasma fibronectin. *Exp. Cell Res.* 165:320–336.
21. Knox, P., and S. Griffiths. 1980. The distribution of cell-spreading activities in sera: a quantitative approach. *J. Cell Sci.* 46:97–112.
22. Lark, M. W., J. Laterra, and L. A. Culp. 1985. Close and focal contact adhesions of fibroblasts to a fibronectin-containing matrix. *Fed. Proc.* 44:394–403.
23. Laterra, J., J. E. Silbert, and L. A. Culp. 1983. Cell surface heparan sulphate mediates some adhesive responses to glycosaminoglycan-binding matrices, including fibronectin. *J. Cell Biol.* 96:112–123.
24. McAbee, D. D., and F. Grinnell. 1983. Fibronectin-mediated binding and phagocytosis of polystyrene latex beads by baby hamster kidney cells. *J. Cell Biol.* 97:1515–1523.
25. McCarthy, J. B., S. T. Hagen, and L. T. Furcht. 1986. Human fibronectin contains distinct adhesion- and motility- promoting domains for metastatic melanoma cells. *J. Cell Biol.* 102:179–188.
26. McKeown-Longo, P. J., and D. F. Mosher. 1985. Interaction of the 70,000-mol-wt amino-terminal fragment of fibronectin with the matrix-assembly receptor of fibroblasts. *J. Cell Biol.* 100:364–374.
27. Merrifield, R. B. 1963. Solid phase peptide synthesis. I. The synthesis of a tetrapeptide. *J. Am. Chem. Soc.* 85:2149–2154.
28. Neyfakh, A. A., Jr., I. S. Tint, T. M. Svitikina, A. D. Bershadsky, and V. I. Gelfand. 1983. Visualization of cellular focal contacts using a monoclonal antibody to 80kD serum protein adsorbed on the substratum. *Exp. Cell Res.* 149:387–396.
28a. Nicol, A., and M. Nermut. 1987. *Eur. J. Cell Biol.* A new type of substratum adhesion structure in NRK cells revealed by correlated interference reflection and electron microscopy. In press.
29. Pierschbacher, M. D., and E. Ruoslahti. 1984. Cell attachment activity of fibronectin can be duplicated by small synthetic fragments of the molecule. *Nature (Lond.).* 309:30–33.
30. Pierschbacher, M. D., E. G. Hayman, and E. Ruoslahti. 1981. Location of the cell-attachment site in fibronectin with monoclonal antibodies and proteolytic fragments of the molecule. *Cell.* 26:259–267.
31. Pierschbacher, M. D., E. G. Hayman, and E. Ruoslahti. 1983. Synthetic peptide with cell attachment activity of fibronectin. *Proc. Natl. Acad. Sci. USA.* 80:1224–1227.
32. Pytela, R., M. D. Pierschbacher, and E. Ruoslahti. 1985. Identification of a 140kD cell surface glycoprotein with properties expected of a fibronectin receptor. *Cell.* 40:191–198.
33. Pytela, R., M. D. Pierschbacher, and E. Ruoslahti. 1985. A 125/115 k-Da cell surface receptor specific for vitronectin interacts with the arginine-glycine-aspartic acid adhesion sequence derived from fibronectin. *Proc. Natl. Acad. Sci. USA.* 82:5766–5770.
34. Reynolds, E. S. 1963. The use of lead citrate at high pH as an electron opaque stain in electron microscopy. *J. Cell Biol.* 17:208–212.
35. Stuchbury, T., M. Shipton, R. Norris, J. P. G. Malthouse, K. Brocklehurst, J. A. L. Herbert, and H. Suschitzky. 1975. A reporter group delivery system with both absolute and selective specificity for thiol groups and an improved fluorescent probe containing the 7-nitrobenzo 2-oxa-1, 3-diazole moiety. *Biochem. J.* 151:417–432.
36. Tarone, G., D. Cirillo, F. G. Giancotti, P. M. Comoglio, and P. C. Marchisio. 1985. Rous sarcoma virus-transformed fibroblasts adhere primarily at discrete protrusions of the ventral membrane called podosomes. *Exp. Cell. Res.* 159:141–157.
37. Thom, D., A. J. Powell, and D. A. Rees. 1979. Mechanisms of cellular adhesion. IV. Role of serum glycoproteins in fibroblast spreading on glass. *J. Cell Sci.* 35:281–305.
38. Vasiliev, J. M. 1985. Spreading of non-transformed and transformed cells. *Biochim. Biophys. Acta.* 780:21–65.
39. Vuento, M., and A. Vaheri. 1979. Purification of fibronectin from human plasma by affinity chromatography under non-denaturing conditions. *Biochem. J.* 183:331–337.
40. Woods, A., M. Höök, L. Kjéllen, C. G. Smith, and D. A. Rees. 1984. Relationship of heparan sulphate proteoglycans to the cytoskeleton and extracellular matrix of cultured fibroblasts. *J. Cell Biol.* 99:1743–1755.
41. Woods, A., C. G. Smith, D. A. Rees, and G. Wilson. 1983. Stages in specialisation of fibroblast adhesion and deposition of extracellular matrix. *Eur. J. Cell Biol.* 32:108–116.
42. Woods, A., J. R. Couchman, S. Johansson, and M. Hook. 1986. Adhesion and cytoskeletal organization of fibroblasts in response to fibronectin fragments. *EMBO (Eur. Mol. Biol. Organ.) J.* 55:665–670.
43. Yamada, K. M. 1983. Cell surface interactions with extracellular materials. *Annu. Rev. Biochem.* 52:761–777.
44. Yamada, K. M., and D. W. Kennedy. 1984. Dualistic nature of adhesive protein function: fibronectin and its biologically active peptide fragment can autoinhibit fibronectin function. *J. Cell Biol.* 99:29–36.